

## Measurement of vacancy transfer probability from K to L shell using K-shell fluorescence yields

Ö SÖĞÜT<sup>1,\*</sup>, E BÜYÜKKASAP<sup>2</sup>, A KÜÇÜKÖNDER<sup>1</sup> and T TARAKÇIOĞLU<sup>1</sup>

<sup>1</sup>Department of Physics, Faculty of Science and Letters, Kahramanmaraş Sütçü İmam University, 46100 Kahramanmaraş, Turkey

<sup>2</sup>Erzincan University Rectorate, Erzincan, Turkey

\*Corresponding author. E-mail: os4fg@yahoo.com

MS received 8 April 2008; accepted 17 February 2009

**Abstract.** The vacancy transfer probabilities from K to L shell through radiative decay,  $\eta_{KL}$ , have been deduced for the elements in the range  $19 \leq Z \leq 58$  using K-shell fluorescence yields. The targets were irradiated with  $\gamma$  photons at 59.5 keV from a 75mCi <sup>241</sup>Am annular source. The K X-rays from different targets were detected with a high resolution Si(Li) detector. The measurement of vacancy transfer probabilities are least-squared fitted to second-order polynomials to obtain analytical relations that represent these probabilities as a function of atomic number. The obtained results agree with theoretical and fitted values.

**Keywords.** Emission probability; Auger effect; photon interaction with atoms; vacancy; Coster–Kronig.

**PACS Nos** 32.30.-r; 32.30.Rj; 32.80.Fb

### 1. Introduction

When a single vacancy is created in an inner shell (e.g. the K-shell), the vacancy will be rapidly filled up ( $10^{-8}$  s) by an electron coming from some higher (sub)shell, so that in a radiative decay a photon and in a radiationless (Auger) decay an electron is emitted. Reliable accurate values of the decay probabilities are required in order to derive the vacancy creation from the observed photons or electrons. To estimate this contribution, knowledge of K to L shell vacancy transfer probabilities is required. However, knowledge of average vacancy distribution is also important for the study of processes such as nuclear electron capture, interval conversion of  $\gamma$ -rays, photoelectric effect and generally, whenever primary vacancies produced in the shell must be distinguished from multiple ionization due to the decay of inner vacancy [1]. The K X-ray production cross-sections and fluorescence yields were measured experimentally [2–4]. Puri *et al* [5,6] have measured K to L shell and L to M shell vacancy transfer probabilities for elements in the atomic range  $37 \leq Z \leq 42$  and  $18 \leq Z \leq 96$ , respectively. Puri *et al* [6] have calculated values

and fitted coefficients for vacancy transfer probabilities of K to L<sub>1</sub>, K to L<sub>2</sub>, K to L<sub>3</sub>, K to L (average), L<sub>1</sub> to M, L<sub>2</sub> to M and L<sub>3</sub> to M shells. K-shell fluorescence yields, mean L-shell fluorescence yields, ratios of X-ray emission probabilities and ratios of emission probabilities of Auger electrons were collected from the literature and evaluated by Schönfeld and JanBen [7]. The variation of the chemical effect of K-shell fluorescence yield and K<sub>β</sub>/K<sub>α</sub> X-ray intensity ratios were studied in refs [8–13]. The K-shell fluorescence yield is also defined as the probability that one K hole is filled through by radiative electron transition and is equal to the ratio of the X-ray emission rate to the total decay:

$$\omega_K = \frac{S_K^{\text{Rad}}}{(S_K^{\text{Rad}} + S_K^{\text{Auger}})}, \quad (1)$$

where  $S_K^{\text{Rad}}$  and  $S_K^{\text{Auger}}$  are the total radiative and Auger transition rates, respectively. The fluorescence yields lie between 0 and 1. For low atomic number elements, Auger decay rate is larger than X-ray emission. For high atomic number, X-ray emission becomes more probable. Auger transition probability increases with decreasing binding energy of the outer shell electrons. Ertuğrul [13] has measured total radiative and radiationless vacancy transfer probabilities from K to L<sub>i</sub> subshell for some elements in the medium atomic number region. The vacancy transfer probabilities in the atomic shell have been studied by a few authors [14–17]. Some authors have measured K to L shell vacancy transfer probabilities using different processes [18–20].

In this study, the vacancy transfer probabilities from K to L shell were experimentally determined using K-shell fluorescence yields for some elements in the atomic number range  $19 \leq Z \leq 58$ .

## 2. Experimental

The experimental arrangement is shown in figure 1. The typical K X-ray spectrum obtained from Mo is given in figure 2. The studied elements are K, Ca, Ti, V, Cr, Mn, Fe, Co, Ni, Cu, Zn, As, Se, Sr, Mo, Ag, Cd, Ba, La and Ce. High purity (99%) samples of thickness  $2\text{--}4 \times 10^{-2} \text{ g cm}^{-2}$  were used for the preparation of the targets. In the experimental set-up, 59.5 keV  $\gamma$ -rays emitted from a 75 mCi <sup>241</sup>Am radioisotope source were detected by a calibrated Si(Li) detector (FWHM = 155 eV at 5.96 keV, active area = 12.5 mm<sup>2</sup>, sensitive depth = 3.5 cm, Be window thickness = 12.5  $\mu\text{m}$ ) and a system 100 card with pulse height analyzer was used to count K<sub>α</sub> and K<sub>β</sub> photons emitted from samples. But, 59.5 keV photons emitted by a 100 mCi <sup>241</sup>Am annular radioactive source were used to stimulate K and Ca samples. The fluorescence K X-rays from the sample were detected by using a collimated Ultra-LEGe detector having a thickness of 5 mm and an energy resolution of 0.150 keV at 5.96 keV. The output from the pre-amplifier, with a pulse pile-up rejection capability, was fed to a multi-channel analyser interfaced with a personal computer provided with suitable software for data acquisition and peak analysis. The net peak area of the K X-rays of each target was determined after background subtraction, tailing and escape peak corrections [21].

Measurement of vacancy transfer probability from K to L shell

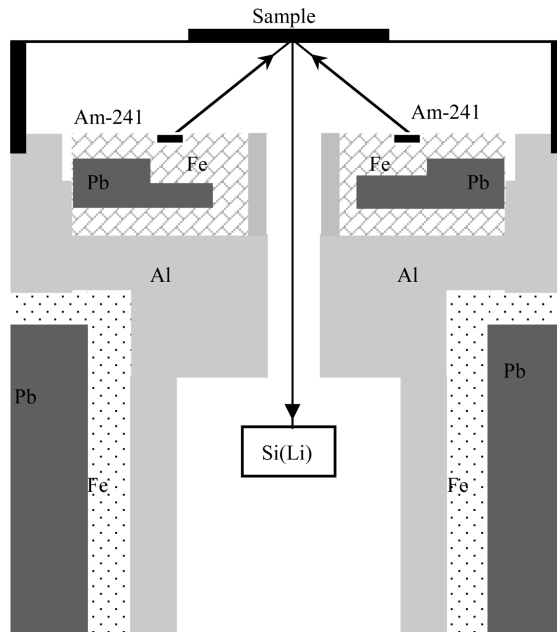


Figure 1. Experimental set-up.

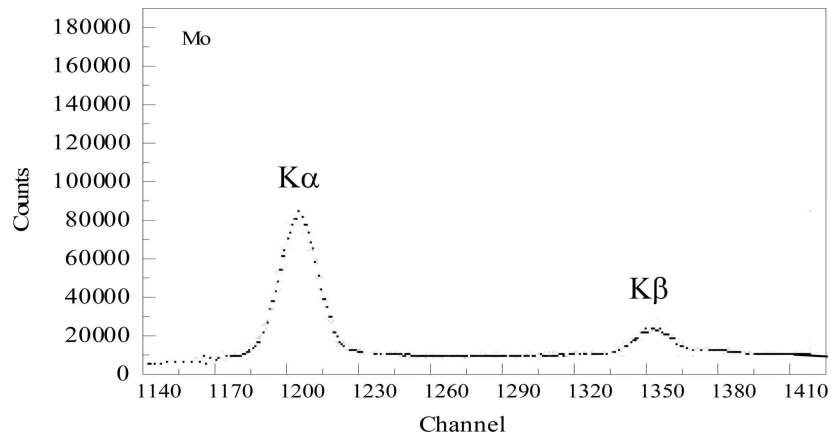


Figure 2. Characteristic K X-ray emission spectrum of Mo.

2.1 Measurement of K-shell fluorescence yield

K-shell fluorescence yield  $\omega_K$  is determined using the following equation semi-empirically [5]:

$$\omega_K = \frac{\sigma_{K\alpha, K\beta}}{\sigma_K^{\text{Photo}}}, \quad (2)$$

where  $\sigma_{K_\alpha, K_\beta}$  is the total K X-ray fluorescence cross-section and  $\sigma_K^{\text{photo}}$  is the K-shell photoionization cross-section [22]. Experimental X-ray fluorescence cross-sections  $\sigma_{K_\alpha}$  and  $\sigma_{K_\beta}$  were determined using the equation [5],

$$\sigma_{K_i} = \frac{N_{K_i}}{I_0 G \varepsilon_{K_i} \beta t}, \quad (3)$$

where  $N_{K_i}$  ( $i = \alpha, \beta$ ) is the intensity observed for  $K_i$  ( $i = \alpha, \beta$ ) X-ray line of element,  $\varepsilon_{K_i}$  is the detector efficiency for  $K_i$  X-rays,  $I_0$  is the intensity of exciting radiation,  $G$  is the geometrical factor,  $t$  is the thickness of the sample in  $\text{g cm}^{-2}$  and  $\beta$  is the self-absorption correction factor of the target material. The self-absorption correction factor has been calculated using the following expression obtained by assuming the incidence angle of the fluorescent X-rays subtended at the detector to be approximately  $90^\circ$  [13].

$$\beta = \frac{1 - \exp[-(-1)(\mu_{\text{inc}}/\cos \varphi + \mu_{\text{emt}})t]}{(\mu_{\text{inc}}/\cos \varphi + \mu_{\text{emt}})t}, \quad (4)$$

where  $\mu_{\text{inc}}$  ( $\text{cm}^2 \text{g}^{-1}$ ) and  $\mu_{\text{emt}}$  ( $\text{cm}^2 \text{g}^{-1}$ ) are the mass absorption coefficients [23] at the incident photon energy and fluorescent X-ray energy of the sample respectively and  $t$  ( $\text{g cm}^{-2}$ ) is the measured thickness of the sample.  $I_0 G \varepsilon_{K_i}$  values in the present experimental set-up were determined in a separate experiment. Targets of pure elements, having areas of cross-section similar to those used in the main experiment, with atomic number  $19 \leq Z \leq 58$ , emitting fluorescent radiation in the energy range 3.313–35 keV were irradiated in the same geometry and fluorescent radiation were counted.  $I_0 G \varepsilon_{K_i}$  values for the present set-up were determined by the following equation [13]:

$$I_0 G \varepsilon_{K_i} = \frac{N_{K_i}}{\sigma_{K_i} \beta t}, \quad (5)$$

where  $N_{K_i}$  is the number of counts under the  $K_\alpha$  or  $K_\beta$  peaks and  $\sigma_{K_i}$  is the photoionization cross-section [22]. The experimental probabilities of total vacancy transfer ( $\eta_{\text{KL}}$ ) from K to L shell were evaluated from [7]

$$\eta_{\text{KL}} = \frac{2 - \omega_K}{1 + \left(\frac{IK_\beta}{IK_\alpha}\right)}, \quad (6)$$

where  $\omega_K$  is the experimental K-shell fluorescence yield and  $IK_\beta/IK_\alpha$  is the intensity ratios of K X-rays [24].

### 3. Results and discussion

The experimental results along with the theoretically calculated values are presented graphically as vacancy transfer probabilities vs. atomic numbers in figure 3 from which we observe that the values of  $\eta_{\text{KL}}$  decrease as the atomic numbers increase. The experimental and theoretical vacancy transfer probabilities are listed

Measurement of vacancy transfer probability from K to L shell

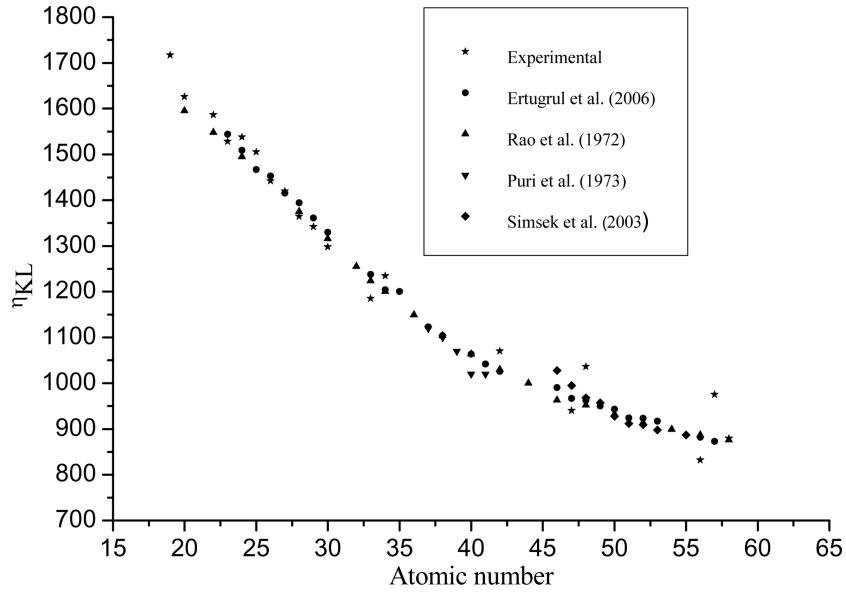


**Figure 3.** Total vacancy transfer probabilities of K to L shell as a function of atomic number.

in table 1. The overall error of these measurements is estimated to be 6–10%. The error in the evaluation of peak areas is 3%, the target thickness is  $\leq 1\text{--}2\%$ ,  $I_0G$  product is 1–2% and the error in the absorption factor is  $\leq 1\text{--}3\%$ . It can be seen from table 1 and figure 3 that our measurement values are in good agreement, within experimental uncertainties, with the calculated theoretical values for the elements in the atomic range  $19 \leq Z \leq 58$ .

Our experimental values were fitted to a second-order polynomial as a function of atomic number  $Z(\Sigma A_n Z^n)$  and fitted values of the K to L shell vacancy transfer probability are listed in table 1. These values have been plotted as a function of the atomic number and are shown in figure 3. The fitted equation is given as  $Y(Z) = 2616.32434 - 57.7968Z + 0.48698Z^2$ ,  $R^2 = 0.98054$  and  $SD = 40.11375$ .

As seen from table 1, the present values of  $\eta_{KL}$  are in good agreement (1–4%) with fitted values of Schönfeld and JanBen [7] (except for Sr and Fe) and the values of Ertugrul *et al* and Şimşek and JanBen [14,25]. But, our fitted values are 1–3% different from Schönfeld's values [7]. Schönfeld and JanBen have evaluated the emission probabilities of X-rays and Auger electrons emitted in radioactive disintegration processes [26]. Furthermore, the probabilities of radiative vacancy transfer from  $L_i$  ( $i = 1, 2, 3$ ) subshells to the M, N and higher shells for elements with  $77 \leq Z \leq 92$  have been measured by Sharma *et al* [20]. In addition, Çalışkan *et al* have measured the radiative vacancy distributions for the  $L_2, L_3$  subshell and M shell of some elements in the atomic range  $41 \leq Z \leq 68$  [27]. In early measurements [6,14,18] the authors used two radioisotope sources for the excitation of samples to determine the K to L shell vacancy transfers experimentally. This method was based on the number of L X-rays produced at the photon excitation energy below the K edge and at the excitation energy above the K edge, where the major contribution

**Table 1.** Comparison of experimental and theoretical results for K to L shell vacancy transfer probabilities.

Element	$\eta_{KL}$						Fit values
	Experimental	Ertuğrul <i>et al</i> [25]	Rao <i>et al</i> [1]	Puri <i>et al</i> [6]	Şimşek [14]	Schönfeld and JanBen [7]	
19	1.721±0.153	–	–	–	–	1.654	1.694
20	1.689±0.143	–	1.595	–	–	1.621	1.656
21	–	–	–	–	–	1.594	1.617
22	1.586±0.127	–	1.548	–	–	1.566	1.581
23	1.528±0.122	1.544	–	–	–	1.539	1.545
24	1.538±0.123	1.509	1.495	–	–	1.508	1.510
25	1.505±0.120	1.467	–	–	–	1.478	1.476
26	1.442±0.144	1.453	1.139	–	–	1.447	1.443
27	1.420±0.142	1.415	–	–	–	1.418	1.411
28	1.364±0.123	1.394	1.375	–	–	1.388	1.380
29	1.342±0.121	1.361	–	–	–	1.357	1.350
30	1.298±0.104	1.330	1.316	–	–	1.326	1.321
31	–	–	–	–	–	1.294	1.293
32	–	–	1.255	–	–	1.263	1.266
33	1.185±0.083	1.238	1.224	–	–	1.232	1.239
34	1.235±0.099	1.204	1.200	–	–	1.202	1.214
35	–	1.200	–	–	–	1.174	1.190
36	–	–	1.149	–	–	1.149	1.167
37	–	1.123	–	1.120	–	1.125	1.145
38	1.341±0.107	1.104	1.104	1.100	–	1.102	1.123
39	–	–	–	1.070	–	1.081	1.103
40	–	1.064	1.064	1.030	–	1.062	1.084
41	–	1.042	–	1.020	–	1.045	1.065
42	1.070±0.097	1.026	1.030	1.020	–	1.029	1.048
43	–	–	–	–	–	1.014	1.032
44	–	–	1.000	–	–	1.000	1.016
45	–	–	–	–	–	0.987	1.001
46	–	0.990	0.963	–	1.028	0.975	0.988
47	0.940±0.080	0.967	–	–	0.995	0.964	0.976
48	1.036±0.104	0.962	0.952	–	0.968	0.953	0.964
49	–	0.950	–	–	0.957	0.944	0.954
50	–	0.943	0.932	–	0.928	0.934	0.944
51	–	0.924	–	–	0.912	0.925	0.935
52	–	0.923	0.914	–	0.909	0.917	0.928
53	–	0.917	–	–	0.898	0.909	0.921
54	–	–	0.899	–	–	0.902	0.915
55	–	–	–	–	0.887	0.895	0.911
56	0.832±0.042	0.882	0.887	–	–	0.888	0.907
57	0.975±0.060	0.873	–	–	–	0.882	0.904
58	0.879±0.079	–	0.876	–	–	0.876	0.902

to L shell vacancies comes from the decay of K shell vacancies. Consequently, their methods strongly depend on the L X-ray cross-sections. Moreover, the vacancy transitions from K to L shell enhance the L X-ray cross-sections. In addition, as seen from table 1 and figure 3, radiative vacancy transition probabilities decrease with the increasing atomic number. The reason of this may be that the linewidth increases with the increase in the number of electrons in the external shells.

Consequently, the probabilities of radiative and non-radiative vacancy transfers have been studied extensively but not in the range  $19 \leq Z \leq 58$ . Since the probabilities of radiative and non-radiative vacancy transfers directly depend on the electronic structure of the atom, it is necessary to reinvestigate these probabilities in accordance with the new developments in detection system technology.

## References

- [1] P V Rao, M H Chen and B Craseman, *Phys. Rev.* **A5**, 97 (1972)
- [2] Ö Söğüt, *J. Quant. Spectrosc. Radiat. Transfer* **73(1)**, 63 (2002)
- [3] E Baydaş, Ö Söğüt, Y Şahin and E Büyükkasap, *Spectrochim. Acta Part B* **57(2)**, 375 (2002)
- [4] Ö Söğüt, E Baydaş, E Büyükkasap, A Küçükönder and Y Şahin, *Eur. Phys. J.* **D22**, 13 (2003)
- [5] S Puri, D Mehta, D Chand, S Nirmal and P N Trehan, *Nucl. Instrum. Methods* **B73**, 443 (1993)
- [6] S Puri, D Mehta, D Chand, S Nirmal, J H Hubbell and P N Trehan, *Nucl. Instrum. Methods* **B83**, 21 (1993)
- [7] E Schönfeld and H JanBen, *Nucl. Instrum. Methods* **A369**, 527 (1996)
- [8] Ö Söğüt, E Büyükkasap and H Erdoğan, *Chem. Radiat. Phys. Chem.* **64**, 343 (2002)
- [9] Ö Söğüt, E Baydaş, S Seven, E Büyükkasap and A Küçükönder, *Spectrochim. Acta Part B* **56**, 1367 (2001)
- [10] Ö. Söğüt, E Büyükkasap, A Küçükönder, M Ertuğrul and Ö Şimşek, *Appl. Spectrosc. Rev.* **30(3)**, 175 (1995)
- [11] M Ertuğrul, Ö Söğüt, Ö Şimşek and E Büyükkasap, *J. Phys. B: At. Mol. Opt. Phys.* **34**, 909 (2001)
- [12] B Ertuğral, G Apaydın, U Çevik, M Ertuğrul and A İ Kobya, *Radiat. Phys. Chem.* **76(1)**, 15 (2007)
- [13] M Ertuğrul, *Spectrochim. Acta* **B57**, 63 (2002)
- [14] Ö Şimşek, *J. Phys. B: At. Mol. Opt. Phys.* **35**, 1045 (2002)
- [15] Ö. Şimşek, D Karagöz and M Ertuğrul, *Spectrochim. Acta, Part B* **58**, 1859 (2003)
- [16] M Ertuğrul, *J. Phys. B: At. Mol. Opt. Phys.* **36**, 2275 (2003)
- [17] M Ertuğrul, *Nucl. Instrum. Methods Sec.* **B111**, 229 (1996)
- [18] B Ertuğrul, U Çevik, E Tıraoğlu, A I Kopya, M Ertuğrul and O Doğan, *J. Quant. Spectrosc. Radiat. Transfer* **78**, 163 (2003)
- [19] M Ertuğrul, O Doğan and Ö Şimşek, *Radiat. Phys. Chem.* **49**, 221 (1997)
- [20] M Sharma, S Kumar, P Singh, S Puri and N Singh, *J. Phys. Chem. Solids* **66**, 2220 (2005)
- [21] Y Şahin, R Durak, Y Kurucu and S Erzenoğlu, *J. Radioanal. Chem.* **177(2)**, 403 (1994)
- [22] J H Scofield, *Theoretical photoionisation cross-sections from 1 to 1500 keV* (Lawrence Livermore Laboratory, Livermore UCRL-51326, 1973)

- [23] J H Hubbell and S M Seltzer, Tables of X-ray mass attenuation coefficient and mass energy absorption coefficients 1 keV to 20 MeV for elements  $Z = 1$  to 92 and 48 additional substances of dosimetric interest, U.S. Department of Commerce, Technology Administration, National Institute of Standards and Phys. Laboratory NISTIR 5692 (1995)
- [24] J H Scofield, *At. Data Nucl. Data Tables* **14**, 121 (1974)
- [25] B Ertuğrul, G Apaydın, A Tekbıyık, E Tıraşođlu, U Çevik, A İ Kopya and M Ertuğrul, *Eur. Phys. J.* **D37**, 371 (2006)
- [26] E Schönfeld and H JanBen, *Appl. Radiat. Isotopes* **52**, 595 (2000)
- [27] B Çalışkan, M Ertuğrul, E Öz and H Erdoğan, *J. Quant. Spectrosc. Radiat. Transfer* **74(2)**, 139 (2002)